On the Numerical Inversion of Laplace Transforms: Comparison of Three New Methods on Characteristic Problems from Applications

DEAN G. DUFFY
Laboratory for Atmospheres, NASA / Goddard Space Flight Center

Three frequently used methods for numerically inverting Laplace transforms are tested on complicated transforms taken from the literature. The first method is a straightforward application of the trapezoidal rule to Bromwich's integral. The second method, developed by Weeks [22], integrates Bromwich's integral by using Laguerre polynomials. The third method, devised by Talbot [18], deforms Bromwich's contour so that the integrand of Bromwich's integral is small at the beginning and end of the contour. These methods are also applied to joint Laplace-Fourier transform problems. All three methods give satisfactory results; Talbot's, however, has an accurate method for choosing required parameters.

Categories and Subject Descriptors: F.2.1 [**Analysis of Algorithms and Problem Complexity**]: Numerical Algorithms and Problems

General Terms: Algorithms, Measurement

1. INTRODUCTION

Laplace transforms are powerful tools used primarily to solve differential equations. The principal difficulty in using them is finding their inverses. Unless the transform is given in a table, an integration must be performed in the complex plane (Bromwich's integral) to find the inverse. Despite the power of complex analysis, this analytical technique often fails and Bromwich's integral must, finally, be integrated numerically.

There are many numerical techniques available to invert Laplace transforms; Davies and Martin [4] have given an excellent review of those available through 1979. The standard method used to test a numerical inversion scheme is to employ a transform whose inverse is known exactly. Although this is acceptable when developing the scheme, such guidance applied to transforms encountered is in general not useful. Most transforms contain both poles and branch points—the poles give the normal mode solutions, while the branch points yield transient solutions. Indeed many transforms exhibit these features (see [13]). Consequently, a better test of an inversion scheme would be to test it on transforms that possess both poles and branch points.

Laplace transforms may also be employed with other transform techniques, such as Fourier or Hankel transforms, to solve partial differential equations. Although one of the transforms may be inverted analytically through the use of the residue theorem, there are numerous problems where both inversions must be performed numerically. Thus, a fast, accurate inversion scheme for one transform used in conjunction with numerical inversion of the other transform is highly desirable. Consequently, another practical test, similar to using transforms that possess both poles and branch points, might be its suitability for use with numerical inversion schemes for other types of transforms.

The purpose of this paper is to test whether three popular methods of inversion are useful and accurate in inverting transforms representative of those found in applied problems. All of these schemes numerically integrate Bromwich's integral and are commercially available. The first scheme is a straightforward application of the trapezoidal rule to Bromwich's integral. Although the technique is easy to implement, it may converge slowly (see Crump [3]) due to truncation and discretization errors. For these reasons Honig and Hirdes [10] introduced a correction term that reduces discretization errors and various sequence accelerators (a numerical method used to extrapolate a slowly convergent or even divergent sequence to its limit) to minimize truncation errors.

The second method was first suggested by Weeks [22]. The numerical inversion is obtained as an expansion in orthonormal Laguerre functions. Laguerre functions are used because the quadrature formulas involving them are similar to the Laplace transform operator. Later, the scheme was improved by Lyness and Giunta [12]. In this study we shall use a version that was prepared for commercial use by Garbow et al. [6, 7].

The third method is a trapezoidal integration of Bromwich's integral along a special contour devised by Talbot [18]. He noted that many of the difficulties associated with the truncation error could be avoided if Bromwich's contour was deformed so that it begins and ends in the left side of the s-plane. If the locations of the singularities are known, this scheme may provide accurate results at minimal computational expense. A commercially available version of this scheme was developed by Murli and Rizzardi [14].

In Section 2 we give a brief description of the three numerical schemes that are to be tested. In Section 3 we begin our tests by systematically introducing transforms that have only poles, have both poles and branch points and finally have only branch points. We concentrate on moderate values of time because asymptotic methods may be used for very small and very large times. In Section 4 we use the numerical schemes to invert joint Fourier-Laplace transforms. Our findings are given in Section 5.

2. THE NUMERICAL SCHEMES

In this section we give a brief overview of the numerical schemes that we shall be testing. The first method is a straightforward application of the trapezoidal rule to evaluate Bromwich's integral (see Crump [3]) in order to invert the transform $F(s)$:

$$\tilde{f}(t) = \frac{e^{at}}{T}\left\{\frac{1}{2}\mathrm{Re}[F(a)] + \sum_{n=1}^{M}\left[\mathrm{Re}\left[F\left(a + \frac{n\pi i}{T}\right)\right]\cos\left(\frac{n\pi t}{T}\right)\right.\right.$$
$$\left.\left. - \mathrm{Im}\left[F\left(a + \frac{n\pi i}{T}\right)\right]\sin\left(\frac{n\pi t}{T}\right)\right]\right\} \tag{1}$$

where $\tilde{f}(t)$ is the numerical approximation to the exact inverse $f(t)$. Here the value of parameter a must be greater than the real part of any singularity in $F(s)$, the so-called "Laplace convergence abscissa" σ_0. Equation (1) is computationally expensive because of the large number of trigonometric evaluations. Therefore, it is advantageous to let $t = T$ or $t = T/2$ so that the trigonometric functions may be replaced by numerical values. For example, if $t = T/2$, (1) becomes

$$\tilde{f}(t) = \frac{e^{at}}{2t}\left\{\frac{1}{2}\mathrm{Re}[F(a)] + \sum_{n=1}^{M}(-1)^n\left[\mathrm{Re}\left[F\left(a + \frac{n\pi i}{t}\right)\right]\right.\right.$$
$$\left.\left. + \mathrm{Im}\left[F\left(a + \frac{(2n-1)\pi i}{2t}\right)\right]\right]\right\}. \tag{2}$$

Although (1) may be used without modification, Albrecht and Honig [1] showed that the accuracy may be improved by using the mathematical expression for the discretization error to introduce corrective terms. This is done by fixing the quantity at and computing $\tilde{f}(t)$. Then, by reducing a by one fifth in Eq. (2), the inverse for $\tilde{f}(5t)$ is computed. The inverse with a reduced discretization error is given by $\tilde{f}(t) - e^{-2at}\tilde{f}(5t)$. A difficulty arises if there is a singularity in the right half of the s-plane. Generally, in this case, a must be rather large because when it is reduced by one fifth it may lie to the left of a singularity resulting in a numerical instability. However, for this large value of a, e^{-2at} is usually small and the correction term is small. Consequently, the corrective scheme for these cases is not used. (See Test 5 in the next section.)

The truncation error may be reduced through the use of a sequence accelerator. If a sequence of partial sums of (2) alternate sign, Albrecht and Honig [1] showed that a linear interpolation of the maxima and minima could be used to find the limit as $n \to \infty$; if the sequence was monotonic, then the extreme value was used. Honig and Hirdes [10] also suggested the use of Wynn's epsilon scheme [24; 23, Ch. 6] and a curve fitting scheme.

Recently, Smith and Ford [17] examined several nonlinear transformations that accelerate the convergence of a sequence. They found that the best schemes are Wynn's epsilon scheme [24; 23, Ch. 6] and Levin's u-transformation [11; 23, Sect. 10.5]. It should be noted however that the epsilon scheme is numerically unstable under certain conditions. De Hoog et al. [5] suggested certain modifications of the scheme but they do not eliminate the numerical instability. In the case of Levin's u-transformation, only a limited number of terms may be used because the transformation involves binomial coefficients which become large enough that round-off becomes a problem. Consequently, when there are more than thirty partial sums, we only use the last thirty in the transformation. In the following sections we will test the maximum/minimum method of Albrecht and Honig [1], Wynn's epsilon scheme and Levin's u-transformation.

The second method that we test is based upon expressing the numerical inversion in terms of Laguerre polynomials:

$$\tilde{f}(t) = e^{\sigma t} \sum_{s=0}^{m-1} a_s e^{-bt/2} L_s(bt) \tag{3}$$

where $L_s(\ )$ is the Laguerre polynomial, a_s is a coefficient computed from a line integral in the complex plane that involves the transform, and the parameters $\sigma > \sigma_0$, m and $b > 0$ are to be determined. The software developed by Garbow et al. [7] requires the user to provide σ_0, b, σ, an upper limit m_{top} on possible values of m and a "pseudouniform accuracy" ϵ_{tol} defined as

$$\left| \frac{\tilde{f}(t) - f(t)}{e^{\sigma t}} \right| < \epsilon_{tol}. \tag{4}$$

Of all of these parameters, the choice of σ and b is most flexible. Although Giunta et al. [8] have given some theoretical guidance in the optimal choice of b, there is currently no general software to compute this value. For these reasons, we have performed inversions with a wide range of σ and b.

Weeks' method has one particular advantage over the direct method (as well as Talbot's method presented below); this method returns an explicit form of the approximate solution $\tilde{f}(t)$. Consequently, if the inverse is desired at many values of t, these extra values can be obtained at little additional cost because most of the computational cost is spent in calculating the coefficients of the Laguerre expansion. In the direct (and Talbot's) method, we need to restart for each value of t.

The third method considered here was developed by Talbot [18] who noted that the reason why sequence accelerators must be used with the direct integration of Bromwich's integral lies in the highly oscillatory nature of the successive terms as $n \to \infty$. He developed a scheme that avoided this problem by deforming the Bromwich contour so that it starts and ends in the left half of the s-plane where the exponential e^{st} is very small. This deformation is permissible as long as (1) the new contour encloses all of the singularities of the transform and (2) the absolute value of the transform goes uniformly to zero as $|s| \to \infty$ in half-plane $\mathrm{Re}(s) < \sigma_0$.

Murli and Rizzardi [14] have developed a commercially available version of Talbot's method. In the first portion of the code, a subroutine called TAPAR determines Talbot's contour through the definition of the parameters σ, ν, and λ once the location and nature of the singularities of $F(s)$ are given and the value of time t and the accuracy of the solution is stated. The subroutine TAPAR also gives the number n of terms that are necessary in the integration; theoretically, this should be the minimum number of terms needed to satisfy the desired (input) accuracy. Of these four parameters, we have the greatest flexibility in choosing σ and n. Consequently, in the next section, we perform the inversion with σ, $\sigma/2$ and 2σ given by TAPAR for variable n. In this way we can test the sensitivity of the results to the parameters given by TAPAR.

In the next section, we employ the direct integration, Weeks' method and Talbot's method on five complicated transforms taken from the literature. When the exact solution required a numerical integration of an integral, we used the IMSL routines DQDAGS or DQDAGI [Version 1.1, Jan. 1989], both of which can handle endpoint singularities. The errors associated with these numerical evaluations ranged from $O(10^{-12})$ to $O(10^{-10})$. In the case when the direct integration is applied, we used the code provided by Albrecht and Honig [1] and Honig and Hirdes [10]. Only in the case of Levin's transformation is the code the author's. We obtained a copy of Murli and Rizzardi's [14] and Garbow et al. [7] codes for Talbot's and Weeks' methods, respectively.

3. NUMERICAL TESTS

We apply the numerical inversion schemes presented in the previous section to transforms that are archetypical of those encountered in practice. All computations were done in double precision on an IBM 3081 for two reasons. First, they were sufficiently fast to allow use of a scalar machine; their computational cost is given in Table I. Second, because many investigators have access to scalar but not vector machines, we decided to determine their efficiency on a common mainframe.

Before we began our tests, we checked out the various inversion schemes on the sixteen test transforms suggested by Davies and Martin [4]. The results are summarized in Table II. The error quantities L and L_e are defined as

$$L = \sqrt{\sum_{i=1}^{30} \left[f(t_i) - \tilde{f}(t_i) \right]^2 \Big/ 30} \tag{5}$$

and

$$L_e = \sqrt{\left(\sum_{i=1}^{30} \left[f(t_i) - \tilde{f}(t_i) \right]^2 e^{-t_i} \right) \Big/ \left(\sum_{i=1}^{30} e^{-t_i} \right)} \tag{6}$$

where $t_i = i/2$. We have also given the average inversion time in μs on the IBM 3081.

For the direct method, Eq. (2) was used with $at = 15$, $M = 300$ and Levin's u-transformation to accelerate the convergence of the sum. Generally, the results are good, the greatest failure occurring for the square wave function (Test 12). For Weeks' method, we took $\sigma - \sigma_0 = \frac{1}{15}$ and $b = \frac{2}{3}$. The results are quite good, except when the inverse has a discontinuity (Tests 10 or 12), $\sqrt{t}$ singularity at the origin (Tests 2, 9, and 14) or a $\ln(t)$ singularity at the origin (Test 11). This is consistent with the findings of Garbow et al. [7]. Finally, the parameters used with Talbot's method were provided by the subroutine

Table I. Average Time for a Single Inversion

	Direct integration	Weeks' method	Talbot's method
Laplace inversion on IBM 3081 in milliseconds			
Test 1	250	71	NA
Test 2	50	93	25
Test 3	14	74	18
Test 4	15	98	26
Test 5	15	80	20
Joint Laplace–Fourier inversion on CRAY Y-MP in seconds			
	Direct integration	Weeks' method	Talbot's method
Test 1	35	49	23
Test 2	72.5	64	12

Table II. Summary of the Errors L and L_e and the Inversion Time τ in μs Associated with the Direct, Weeks and Talbot Techniques for the 16 Transform Tests Given by Davies and Martin [4]

	Direct method			Weeks' method			Talbot's method		
Test	L	L_e	τ	L	L_e	τ	L	L_e	τ
1	5.3(−8)	1.3(−7)	241896	3.6(−8)	4.2(−8)	15314	2 8(−2)	2.9(−2)	1827
2	1.5(−8)	4 0(−8)	232691	1.1(−1)	5.4(−2)	72306	1.3(−11)	3 4(−11)	2011
3	1.2(−8)	8.7(−9)	229956	3.2(−11)	2.4(−11)	2556	4 1(−12)	3.9(−12)	1108
4	9.6(−9)	1.7(−9)	243279	1.5(−15)	1.7(−15)	14046	2 4(−10)	4.2(−12)	1595
5	2.3(−8)	2.1(−8)	211554	1.2(−15)	1.3(−15)	1760	3 9(−12)	3 9(−12)	1093
6	2.1(−9)	4.4(−10)	207070	2.4(−13)	2.2(−13)	1825	7 6(−13)	1.4(−13)	1155
7	4.3(−9)	2.5(−9)	241524	2.6(−11)	1.4(−11)	4281	7.3(−12)	3.0(−13)	1435
8	3.3(−8)	1.6(−9)	231364	6.2(−11)	5.5(−11)	13286	2.4(−11)	3.9(−11)	1550
9	5.1(−9)	1.4(−8)	210836	1.1(−1)	5.4(−2)	57707	1 3(−11)	2.7(−11)	1438
10	1.6(−4)	5.9(−5)	109280	1 2(−2)	6.1(−3)	68439	3.9(−12)	3.9(−12)	1093
11	8.2(−9)	1.3(−8)	177706	7.9(−3)	3.9(−3)	60120	1.1(−11)	1.8(−11)	1438
12	2.2(−3)	1.1(−3)	255003	8.3(−2)	3.9(−2)	68463	—	—	—
13	1 8(−9)	3.1(−9)	107851	1.5(−13)	1.6(−13)	27770	8.6(−12)	3.3(−12)	1812
14	3.2(−9)	7.0(−9)	265870	1.4(−2)	6.8(−3)	64070	1.6(−12)	3.4(−12)	1659
15	4.6(−10)	6.8(−12)	250958	2.9(−9)	3.0(−9)	65577	2.3(−12)	7.8(−12)	1736
16	7.4(−8)	1.7(−8)	410980	5.8(−13)	2.7(−13)	74276	8.3(−10)	8.7(−11)	24990

TAPAR. The results are very good except for Test 1 (the Bessel function $J_0(t)$) for some mysterious reason. The case of the square wave (Test 12) cannot be computed because the poles of this transform have imaginary parts that increase without bound. The transform e^{-5s}/s (Test 10) becomes the same as $1/s$ (Test 5) when the required shifting technique is applied (see [14], Section 4.2).

3.1 Test 1

Our first test is to find the inverse of

$$F(s) = \frac{1}{s(s+c)}\left[\frac{1}{2sh} - \frac{e^{-2sh}}{1-e^{-2sh}}\right] \tag{7}$$

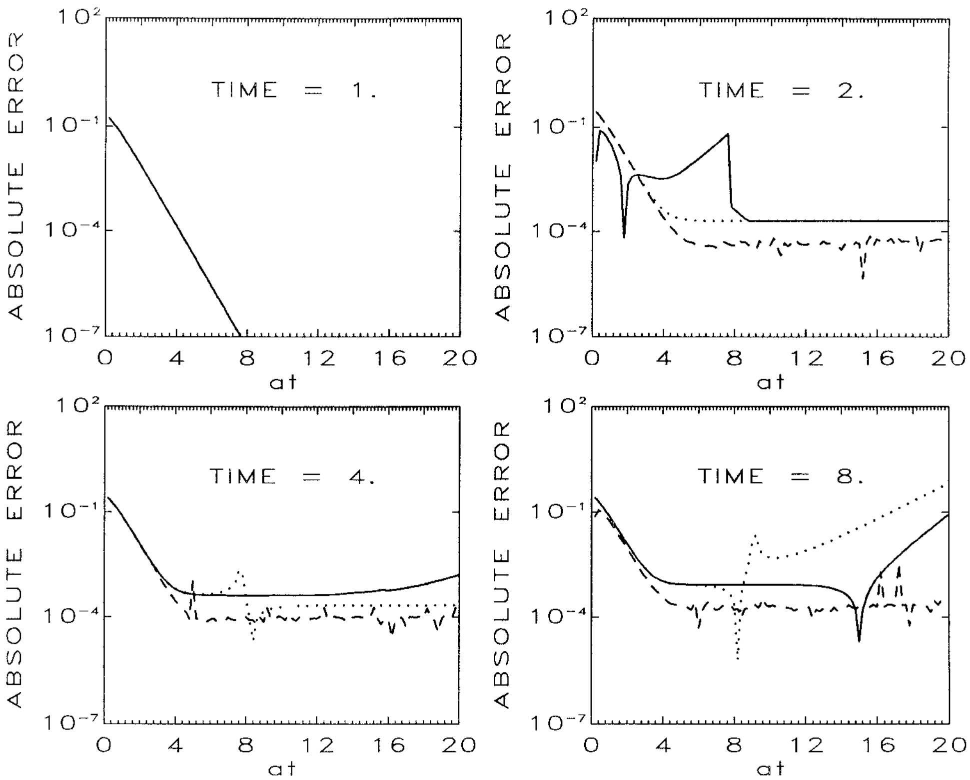

Fig. 1. The absolute value of the error between the direct numerical integration and the actual inverse for various sequence accelerators as a function of at for Test 1. The solid line is for maximum/minimum; the dotted line, the u-transformation and the dashed line, the epsilon scheme. The parameters are $c = h = 1$.

where the parameters c and h are real. This transform [13, Sect. 8.63] arises in circuit theory and has the inverse

$$f(t) = \frac{1}{2c} + \frac{e^{-ct}}{c}\left[\frac{1}{2ch} - \frac{e^{2ch}}{e^{2ch}-1}\right] - \frac{h}{\pi}\sum_{n=1}^{\infty}\frac{\sin\left[\frac{n\pi t}{h} - \tan^{-1}\left(\frac{n\pi}{ch}\right)\right]}{n\sqrt{n^2\pi^2 + c^2h^2}}, \quad (8)$$

where $c > 0$ or $c < 0$. We choose this problem because it does not contain any branch point singularities. Furthermore, the transform and its inverse are similar to those that arise in solutions of the wave equation over a finite domain.

Figure 1 shows the absolute value of the absolute error $|f(t) - \tilde{f}(t)|$ (we note that this error will be presented in subsequent figures) using direct integration for various values of at for times 1, 2, 4, and 8 when $c = h = 1$, $M = 1000$, and when (2) is used. In the evaluation of (8), 10^7 terms were

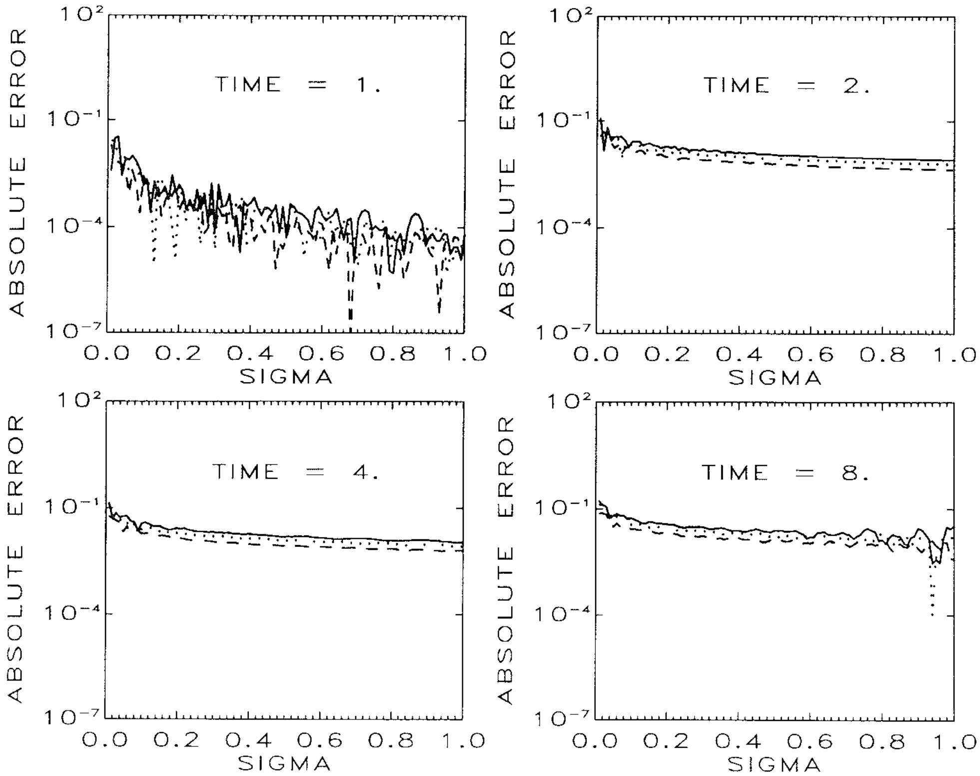

Fig. 2. The absolute value of the error between Weeks' method and the actual inverse as a function of σ given in (3) for Test 1 The solid line is for $b = 3(\sigma - \sigma_0)$; the dotted line, for $b = 5(\sigma - \sigma_0)$ and the dashed line, $b = 10(\sigma - \sigma_0)$. The parameters are $c = h = 1$.

summed; the error associated with these evaluations is $O(10^{-7})$. Despite the large M, the accuracy of the numerical solution is not particularly good; there are two reasons for this. First, unlike most transforms in the literature, we have an infinite number of singularities to resolve rather than just a few. Consequently, for any finite number of terms in the inversion, we badly misrepresent the contribution from the poles far from the origin. Second, these poles lie along the imaginary axis rather than the negative real axis and they represent sinusoidal solutions. Although the contributions of poles far from the origin are not dominant, they do represent higher harmonics which are necessary for accurate results.

Figure 2 shows the error using Weeks' method for various σ at times 1, 2, 4, and 8 when $m_{top} = 1024$, $\epsilon_{tol} = 10^{-10}$, and $\sigma_0 = 0$. Three values of b were tested: $3(\sigma - \sigma_0)$, $5(\sigma - \sigma_0)$, and $10(\sigma - \sigma_0)$. As Figure 2 shows, the results are rather sensitive to the value of b. Finally, Talbot's method cannot be used in this case because the singularities extend along the imaginary axis from $-i\infty$ to $i\infty$, and all of them cannot remain within the modified contour.

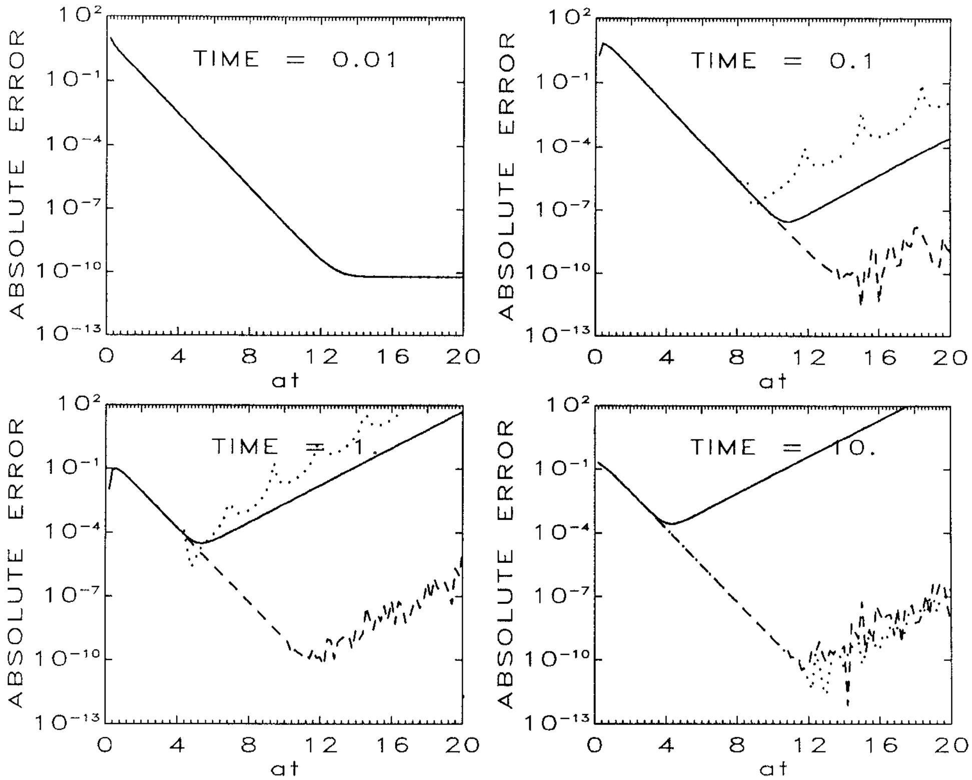

Fig. 3. Same as Figure 1, except for Test 2.

3.2 Test 2

In a study of the longitudinal impact on viscoplastic rods, Ting and Symonds [20] inverted a transform similar to

$$F(s) = \frac{(100s - 1)\sinh(\sqrt{s}/2)}{s[s\sinh(\sqrt{s}) + \sqrt{s}\cosh(\sqrt{s})]}. \tag{9}$$

Although this transform appears to have a branch point at $s = 0$, when the hyperbolic functions are expanded there is only a simple pole at $s = 0$ along with poles lying along the negative real axis at $s = -b_n^2$, where $b_n \tan(b_n) = 1$. The inverse is

$$f(t) = -\frac{1}{2} + \sum_{n=1}^{\infty}\left(100 + \frac{1}{b_n^2}\right)\frac{2b_n \sin(b_n/2)e^{-b_n^2 t}}{(2 + b_n^2)\cos(b_n)}. \tag{10}$$

Figure 3 shows the error for various values of at for times 0.01, 0.1, 1, and 10 for the direct integration method when $M = 100$. Despite the few terms taken, the accuracy is rather good. This occurs because the singularities lie along the negative real axis and yield normal modes that vanish exponen-

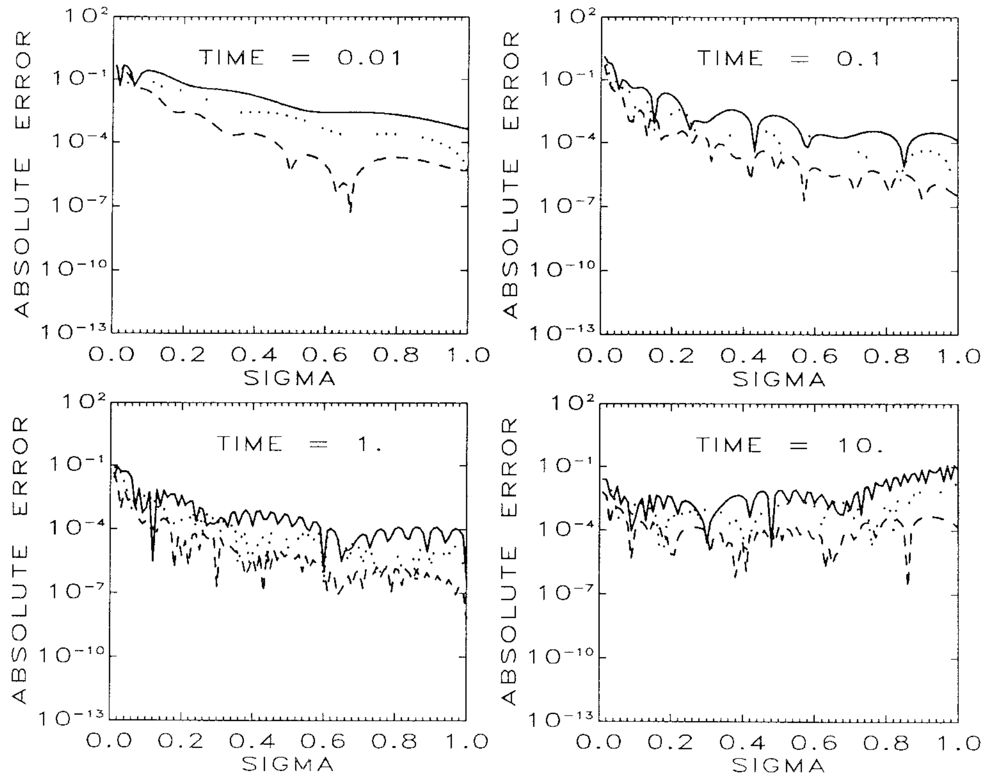

Fig. 4. Same as Figure 2, except for Test 2

tially with time. Consequently, only a few terms in (2) are necessary to capture the most significant singularities which lie near the origin. Figure 4 gives the inversion by Weeks' method for the same parameters given in Test 1. The best results are for large b.

Test 2 provides the first test of Talbot's method. Figure 5 gives the error at times 0.01, 0.1, 1, and 10 as the number of terms in the integration is varied. The values of the parameters σ, ν, and λ are given by the subroutine TAPAR for a specified error of 10^{-10}. Additional calculations were performed with $\sigma/2$ and 2σ; the lines representing $\sigma/2$ and 2σ lie on top of the line for σ. As Figure 5 shows, Talbot's method did extremely well over a wide range of values of n. The TAPAR subroutine predicted that the number of terms needed to achieve the desired accuracy was 18; this was confirmed by the experiment. Similar accurate estimates were found in subsequent tests.

3.3 Test 3

The first test that incorporates both poles and branch points is

$$F(s) = \frac{1}{s}\exp\left\{-r\sqrt{\frac{s(1+s)}{1+cs}}\right\}. \tag{11}$$

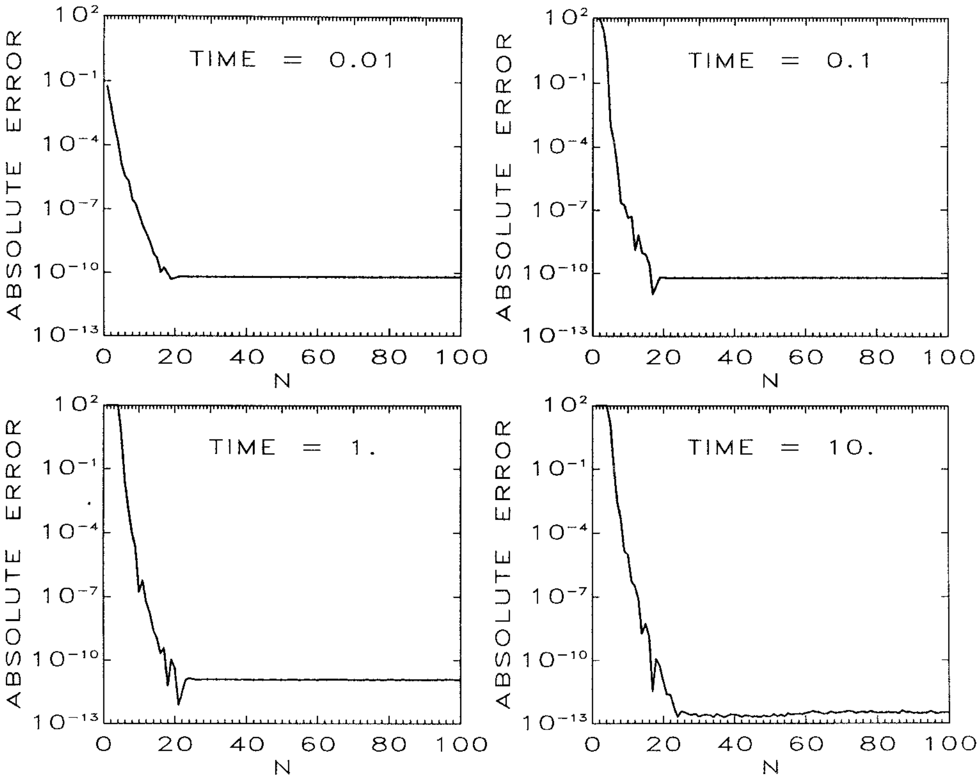

Fig. 5. The absolute value of the error between Talbot's method and the actual inverse as a function of the number n of terms taken in the inversion for Test 2. The solid line is for the parameter σ predicted by subroutine TAPAR; the dotted line, when $\sigma/2$ is used in the subroutine TSUM, and the dashed line, when 2σ is used in TSUM.

This transform arises in a viscous fluid mechanics problem [19]. If the parameter $c = 1$, the inverse is the complementary error function. For $c = 0$, we obtain a solution similar to that describing the distortion of a propagating signal in an infinite transmission line [9, Sect. 10.3]. In general, the solution is

$$f(t) = \frac{1}{2} + \frac{1}{\pi}\int_0^\infty \exp\left[-rm\sqrt{u/2}\,(\cos\theta - \sin\theta)\right]$$
$$\sin\left[tu - rm\sqrt{u/2}\,(\cos\theta + \sin\theta)\right]\frac{du}{u} \tag{12}$$

where

$$m \equiv \left[\frac{1+u^2}{1+c^2u^2}\right]^{1/4} \quad \text{and} \quad 2\theta = \tan^{-1}(u) - \tan^{-1}(cu). \tag{13}$$

The errors for various values of at are shown at times 0.0625, 0.25, 1, and 4 in Figure 6 for the direct integration method when $c = 0.4$, $r = 0.5$, and

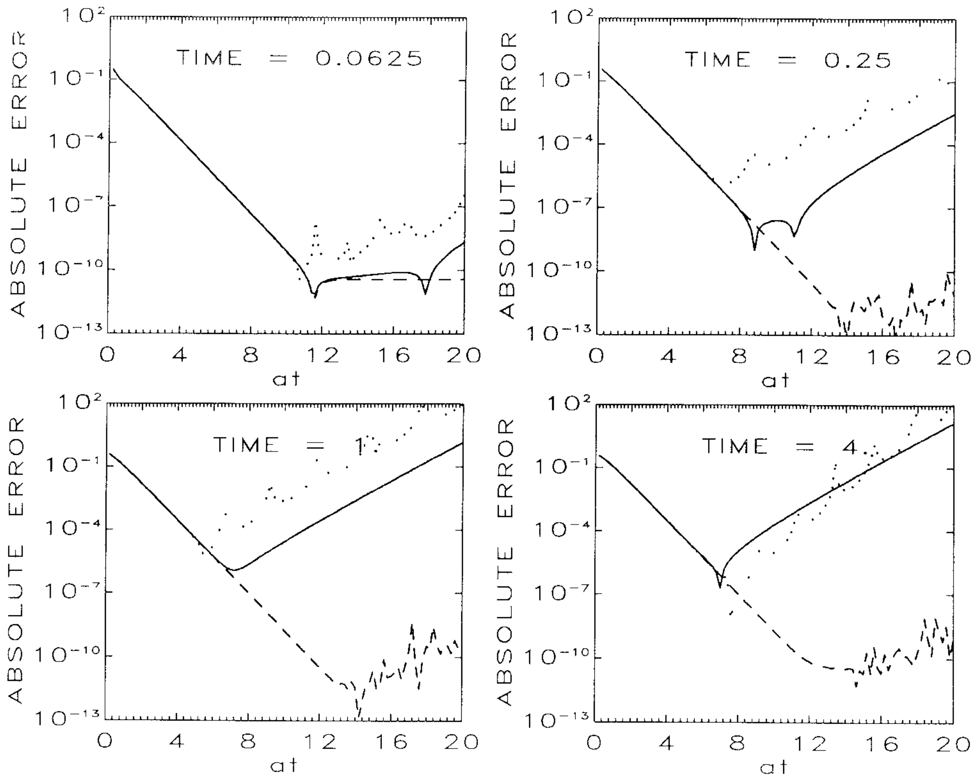

Fig. 6 Same as Figure 1, except for Test 3 Parameters are $c = 0\ 4$ and $r = 0\ 5$

$M = 50$. Despite the relatively few terms used in summing (2), the results are quite good for all of the sequence accelerators. These results are similar to what we would expect if there were no branch points in the transform. Consequently, the location and nature of the poles appears to be the most important factor in determining M rather than the properties of the branch points.

Figure 7 gives the error associated with Weeks' method for the same parameters used in Test 1. The smallest error occurs for the larger values of σ and b. As in the case of direct integration, the accuracy is quite sensitive to the parameters chosen for the inversion scheme. The errors associated with Talbot's method are shown in Figure 8. The same values were found for all values of σ tested. They are very small over a large range of values of n and σ.

3.4 Test 4

Our fourth test is similar to the previous one because it contains poles as well as branch points. However, unlike our previous example, the solutions are not diffusive but are wavelike because they arise in the study of shock waves

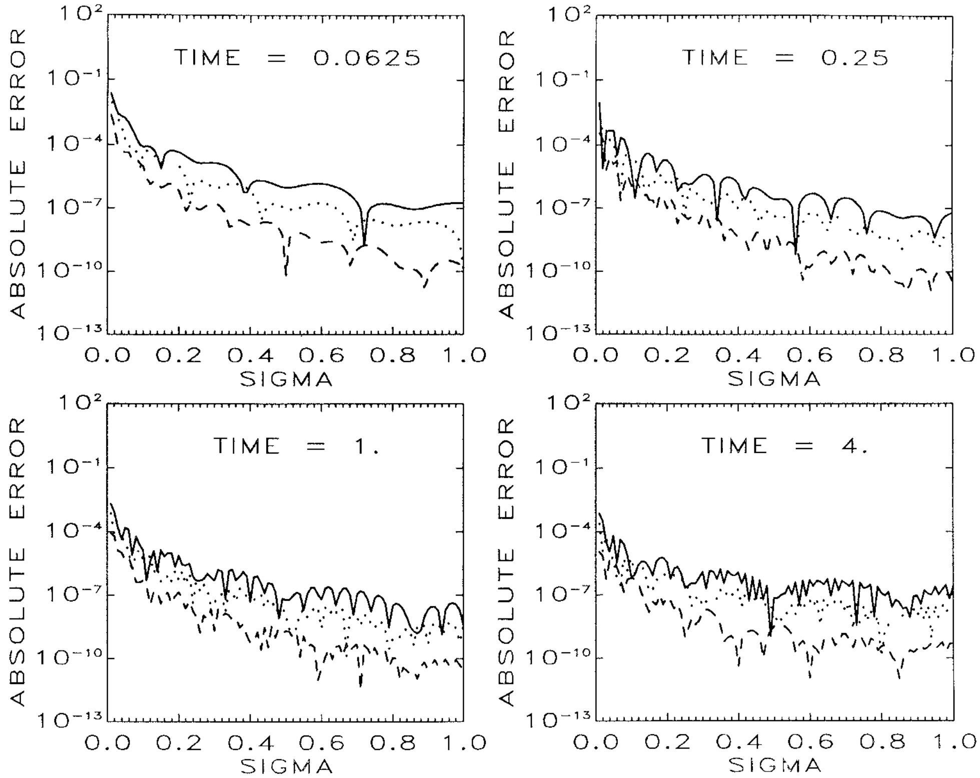

Fig. 7. Same as Figure 2, except for Test 3. Parameters are $c = 0.4$ and $r = 0.5$.

in diatomic chains [15]. The transform is

$$F(s) = \frac{\exp(-2\Psi)}{s} \tag{14}$$

where $\cosh(\Psi) = \sqrt{1 + s^2 + s^4/16}$. The inverse is

$$\begin{aligned} f(t) = 1 &- \frac{1}{\pi}\int_0^{u_1}[\sin(ut + 2k) - \sin(ut - 2k)]\frac{du}{u} \\ &+ \frac{1}{\pi}\int_{u_2}^{4}[\sin(ut + 2k) - \sin(ut - 2k)]\frac{du}{u} \end{aligned} \tag{15}$$

where

$$\cos(k) = \frac{1}{4}\sqrt{(u_1^2 - u^2)(u_2^2 - u^2)}$$

and $u_1 = 2\sqrt{2 - \sqrt{3}}$ and $u_2 = 2\sqrt{2 + \sqrt{3}}$.

Figure 9 shows the error for various at's at times 1, 2, 4, and 8 for the direct integration technique when $M = 50$. Once again, in spite of the six branch points and three branch cuts along the imaginary axis, the results are

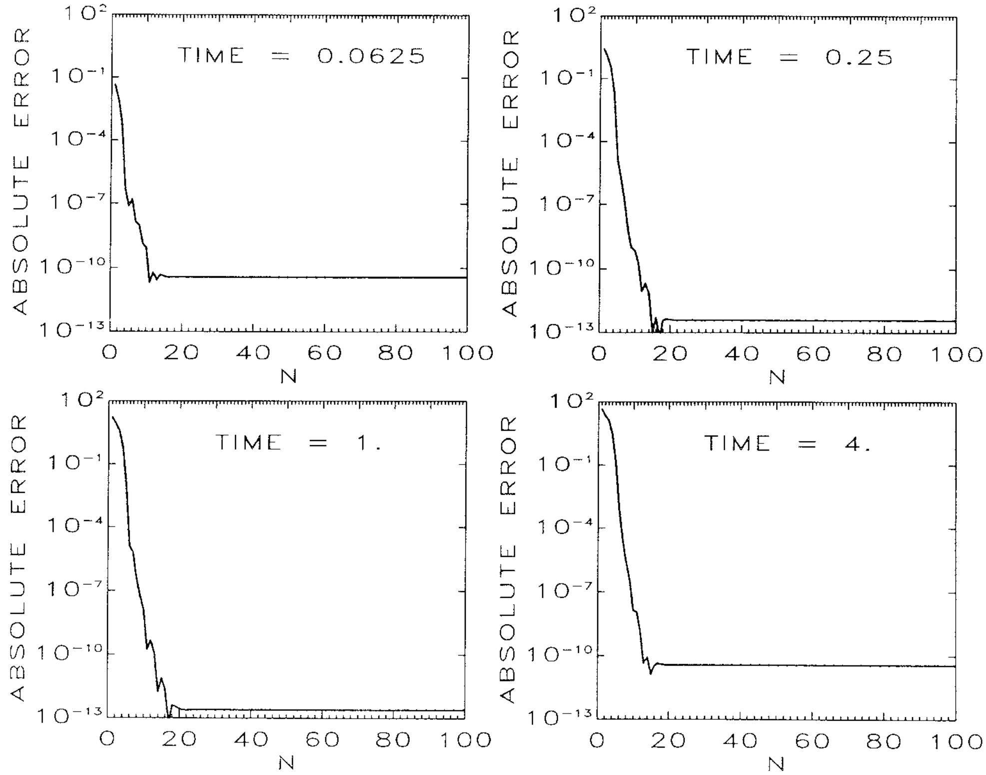

Fig. 8. Same as Figure 5, except for Test 3. Parameters are $c = 0.4$ and $r = 0.5$.

quite good when only relatively few terms are employed. The location and nature of the poles appears to dictate the value of M.

Figure 10 presents the error for Weeks' method. The results are rather insensitive to the value of b and the errors are smallest for $\sigma > 0.3$. The results for Talbot's method are given in Figure 11. This time the results are sensitive to σ, but the errors remain small for a wide range of n.

3.5 Test 5

Our final test arises in the theory of beams [2]. The transform is

$$F(s) = \frac{s - \sqrt{s^2 - c^2}}{\sqrt{s}\,\sqrt{s^2 - c^2}\,\sqrt{s - N\sqrt{s^2 - c^2}}} \qquad (16)$$

where $N < 1$. This transform has five branch points and no poles. Unlike the earlier transformations, it has a singularity in the right half-plane at $s = c$.

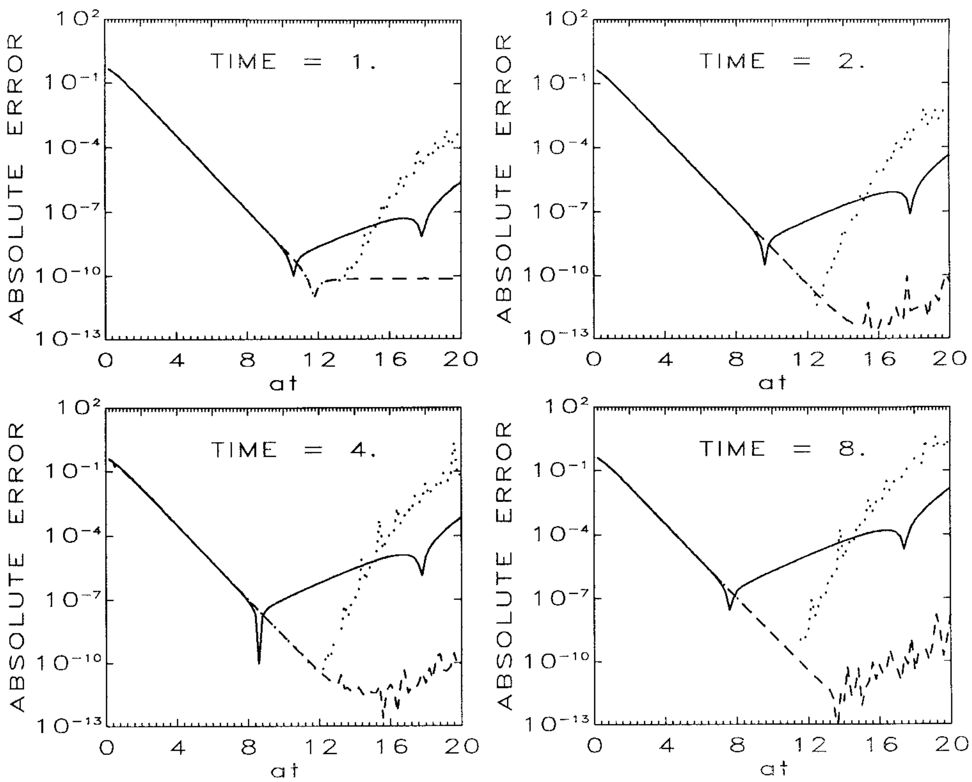

Fig. 9. Same as Figure 1, except for Test 4.

Its inverse is

$$f(t) = \frac{2}{\pi}\int_0^c \cosh(tu)\frac{u\sqrt{(R+u)/2} + \sqrt{c^2-u^2}\sqrt{(R-u)/2}}{R\sqrt{c^2-u^2}\sqrt{u}}du$$
$$+ \frac{2}{\pi}\int_0^b \frac{u-\sqrt{c^2+u^2}}{\sqrt{u}\sqrt{c^2+u^2}\sqrt{N\sqrt{c^2+u^2}-u}}\cos(tu)du \tag{17}$$

where $R = \sqrt{u^2 + N^2(c^2-u^2)}$, $b = \sqrt{(1-N)/(1+N)}$ and $c = (1-N)/N$. Although in this application c is a function of N, the same results would hold if c and N were independent of each other.

Figure 12 shows the error at times $t = 2, 4, 6,$ and 8 for $N = 0.5$ when (2) is used. We have employed fifty terms in the inversion. For reasons stated in the discussion of the direct method in Section 2, we did not use the correction term for the discretization error in the direct method. As Figure 12 shows, all of the sequence accelerators are quite good at the minimum error located near the value $at = 15$.

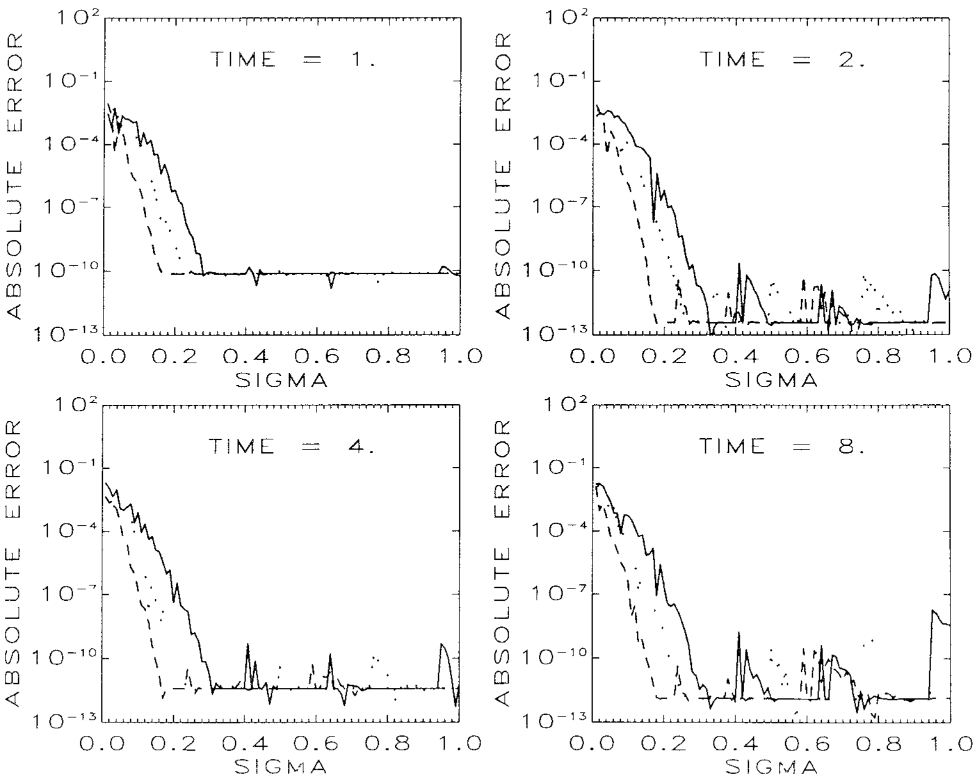

Fig. 10. Same as Figure 2, except for Test 4.

Figure 13 gives the errors associated with Weeks' method with $N = 0.5$. The results are insensitive to b but the best results are obtained for all σ. Figure 14 presents the errors for Talbot's method. For all times, the method does rather poorly.

4. JOINT FOURIER-LAPLACE TRANSFORM

A powerful tool used to solve partial differential equations is the joint application of Fourier and Laplace transforms, especially in elasticity problems. The Fourier transform eliminates the spatial dependence, while the Laplace transform eliminates the temporal dependence. In general, the inversion of both transforms must be performed numerically (see [21] for example). In this section we explore how well the numerical inversion scheme works for this situation. Because the number of calculations is considerable, we performed them on a CRAY Y-MP. Computational costs for these tests are given in Table I. Most of the computational time ($\sim 99\%$) was spent in inverting the Laplace transform because the inversion of the Fourier transform could be

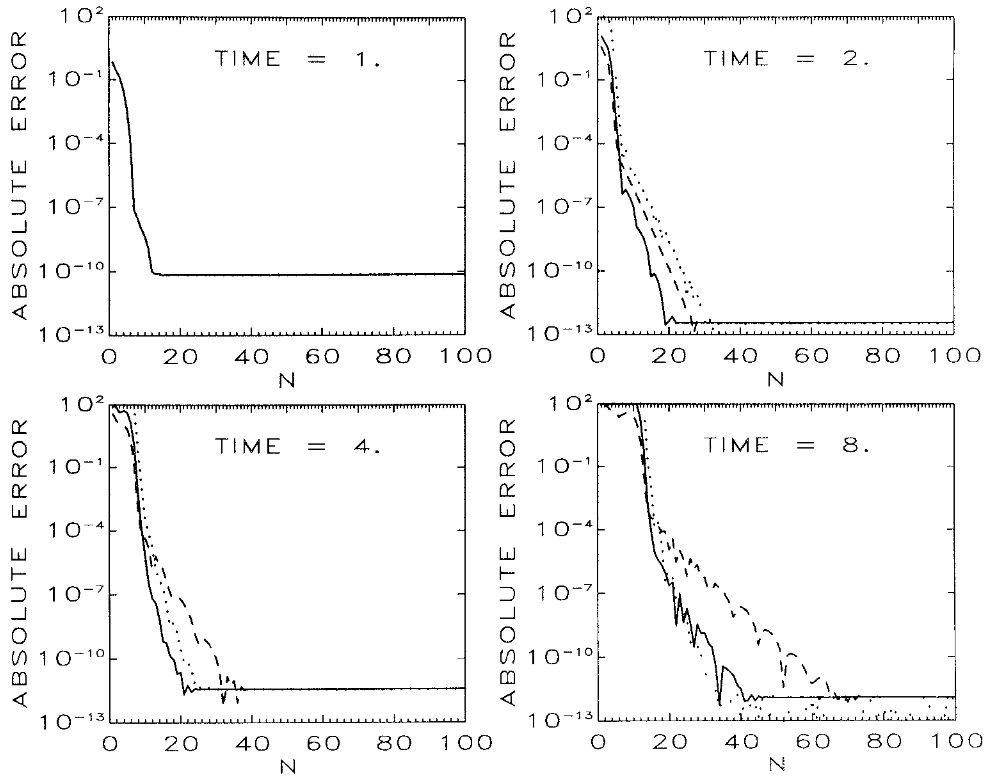

Fig. 11. Same as Figure 5, except for Test 4.

vectorized while the inversion of Laplace transform has a considerable amount of scalar code.

4.1 Test 1

Our first test involves the inversion of the joint Fourier-Laplace transform

$$F(s) = \frac{2}{\pi}\int_0^\infty \frac{\sin(k)\sin(kx)}{k^2 + s^2 + 1}\,dk, \tag{18}$$

which has the inverse

$$f(t) = \frac{2}{\pi}\int_0^\infty \frac{\sin(k)\sin(kx)\sin\left(t\sqrt{k^2+1}\right)}{\sqrt{k^2+1}}\,dk \tag{19}$$

or

$$\begin{aligned} f(t) = {} & \frac{1}{2}J_0\left(\sqrt{t^2-(x-1)^2}\right)H(t-|x-1|) \\ & -\frac{1}{2}J_0\left(\sqrt{t^2-(x+1)^2}\right)H(t-|x+1|) \end{aligned} \tag{20}$$

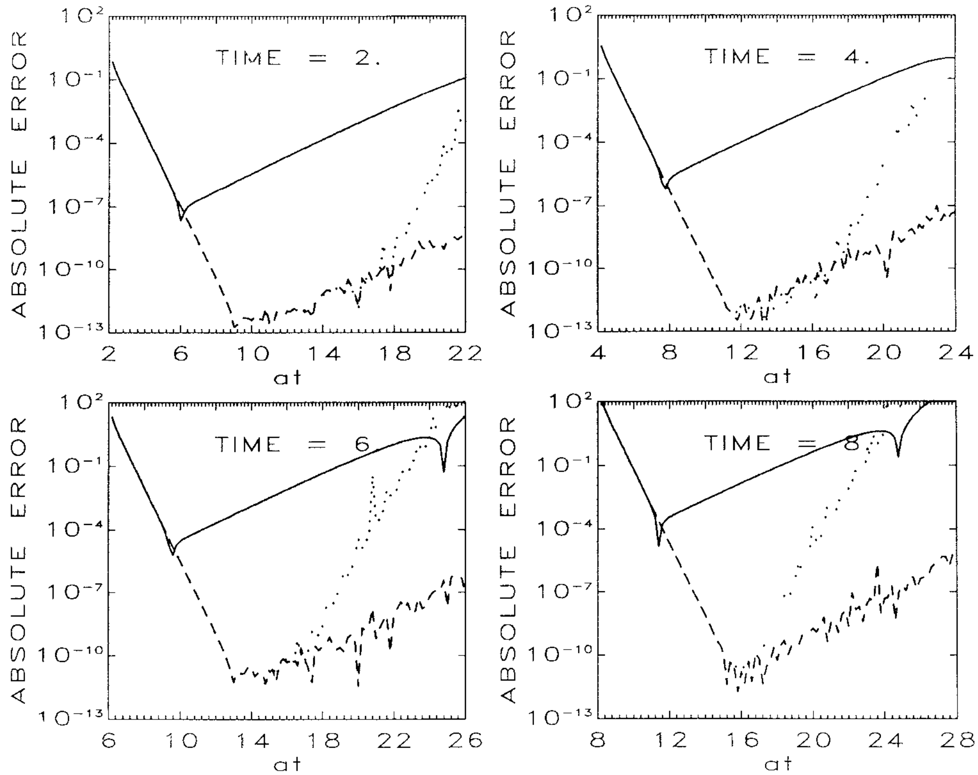

Fig. 12 Same as Figure 1, except for Test 5 with $N = 0.5$.

where $J_0(\ )$ denotes a Bessel function of the first kind and zeroth order, and $H(\ )$ denotes the Heaviside step function. The advantage of this test is that we can find the inverse Laplace transform before we perform the Fourier inversion and see whether the inversion schemes are providing accurate values for the integrand of the Fourier inversion. They did.

All three methods were tested on this joint transform. For Talbot's method, the parameters were chosen by the subroutine TAPAR with the requirement that the error be less than 10^{-10}. Three values of σ were used. Weeks' method was used with $\sigma_0 = 0.$, $\sigma = 0.7$, $\epsilon = 10^{-10}$ and $m_{top} = 1024$, and three different values of b. Finally, the direct integration method used $at = 5$ and $M = 1000$. The correction for the discretization error was always used but one of the tests used no sequence accelerators while the minimum/maximum and u-transformation methods were also tested.

All of the calculations were performed in single precision on a CRAY Y-MP. To take full advantage of vectorization, certain modifications to the code were necessary. Considerable improvement was achieved—typically three times faster than the standard scalar code. Once the code was verified, four time periods were run with $0 < x < 5$ in intervals of 0.1. The Fourier inverse was computed using a sixth-order Cotes scheme with $\Delta k = 0.01$ and $k_{max} = 240$.

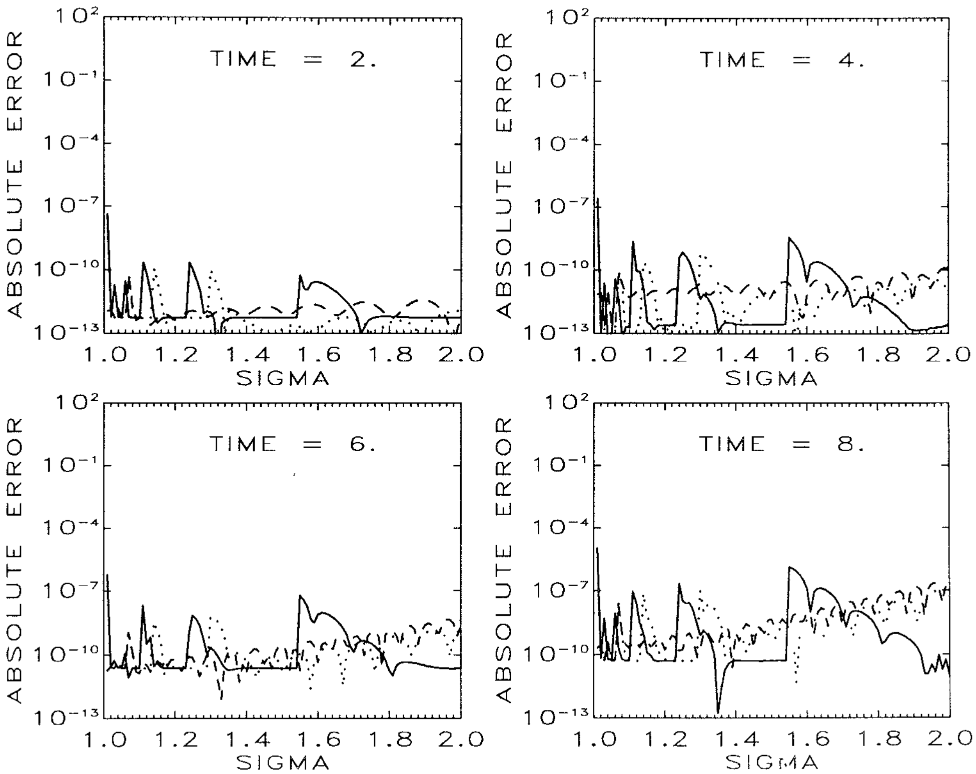

Fig. 13. Same as Figure 2, except for Test 5 with $N = 0.5$.

Figures 15–17 show the absolute error for the direct integration, Weeks' and Talbot's methods, respectively. For the direct integration method the sequence accelerators did little to enhance the accuracy of the final result. The results from Weeks' method are very sensitive to b. The parameters given by TAPAR gave good results in the inversion by Talbot's method.

We note that the error curves in Figure 15 (the direct method) and 17 (the Talbot method) are very similar (but not equal). Because we invert the Laplace transform numerically before we invert the Fourier transform, similar errors could occur if the numerical inversions of the Laplace transform given by the direct and Talbot's methods produce similar results. This is indeed the case for this particular test.

4.2 Test 2

Our second test is much more difficult. It arises in geophysics in the study of Rayleigh waves which are excited by an impulse in an elastic half-plane. After applying the joint transform technique, the Laplace transform of one of the solutions (after some scaling) is

$$F(s) = \int_0^\infty \frac{\nu_\alpha(2k^2 + s^2/\gamma^2)}{G(k)} e^{-\nu_\alpha z} \cos(kx)\,dk \tag{21}$$

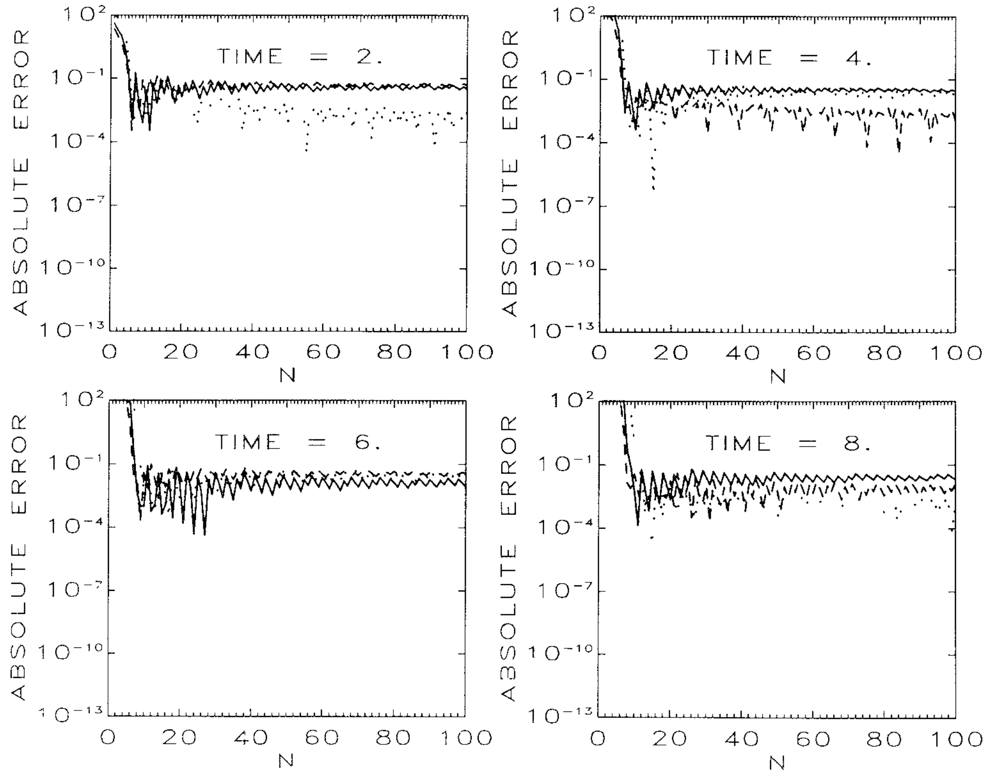

Fig. 14. Same as Figure 5, except for Test 5 with $N = 0$ 5

where

$$G(k) = (2k^2 + s^2/\gamma^2)^2 - 4k^2\nu_\alpha\nu_\beta,$$
$$\nu_\alpha = \sqrt{k^2 + s^2}, \quad \nu_\beta = \sqrt{k^2 + s^2/\gamma^2}. \tag{22}$$

The ratio of the speed of the secondary wave to the primary one is denoted by γ, and the position of the observer by (x, z). As is shown in [16, Sect. 3.2.2], the inverse $f(t)$ is

$$f(t) = \mathrm{Re}\left\{\frac{\cos^2(\theta + i\beta)[1 - 2\gamma^2\sin^2(\theta + i\beta)]}{rG_1\sinh(\beta)}\right\}\gamma^2 H(t - r) \tag{23}$$

where

$$G_1 = [1 + 2\gamma^2\sin^2(\theta + i\beta)]^2 + 4\gamma^3\sin^2(\theta + i\beta)\cos(\theta + i\beta)\sqrt{1 - \gamma^2\sin^2(\theta + i\beta)} \tag{24}$$

and $\beta = \cosh^{-1}(t/r)$, $x = r\sin(\theta)$ and $z = r\cos(\theta)$.

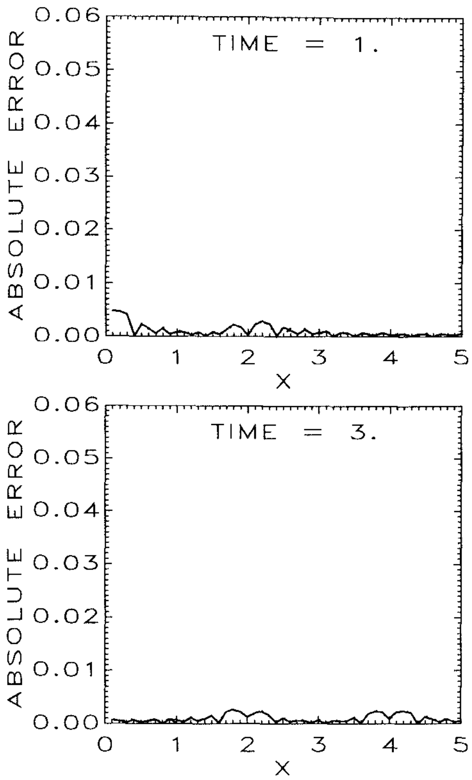

Fig. 15. The absolute value of the error between the direct numerical integration and the actual inverse for (16) as a function of x. The dashed line is the numerical inverse where only the discretization error is corrected; the solid line, both the maximum/minimum sequence accelerator and the discretization error correction are used and the dotted line, both the u-transformation and the discretization error correction are applied.

Figures 18–20 show the absolute error for direct integration, Weeks' and Talbot's methods, respectively, when $z = 1$ and $\gamma^2 = \frac{1}{3}$. The inversion of the Fourier transform now involves $\Delta k = 0.001$ and $k_{max} = 24$. The presence of k in the exponential results in a rapid decrease in the magnitude of the transform for increasing k. The same parameters used in the previous test were used in the present one.

In general, the errors are larger than in the earlier, simpler case. In particular, the use of Levin's u-transformation sequence accelerator in the direct integration resulted in $O(1)$ errors for $t = 2$; these errors were not plotted. Except for this case, all of the schemes gave acceptable results. In general, the relative errors were small except when the magnitude of the solution was small. Consequently, if a high degree of precision in not needed, then our results suggest that these inversion schemes are acceptable. On the

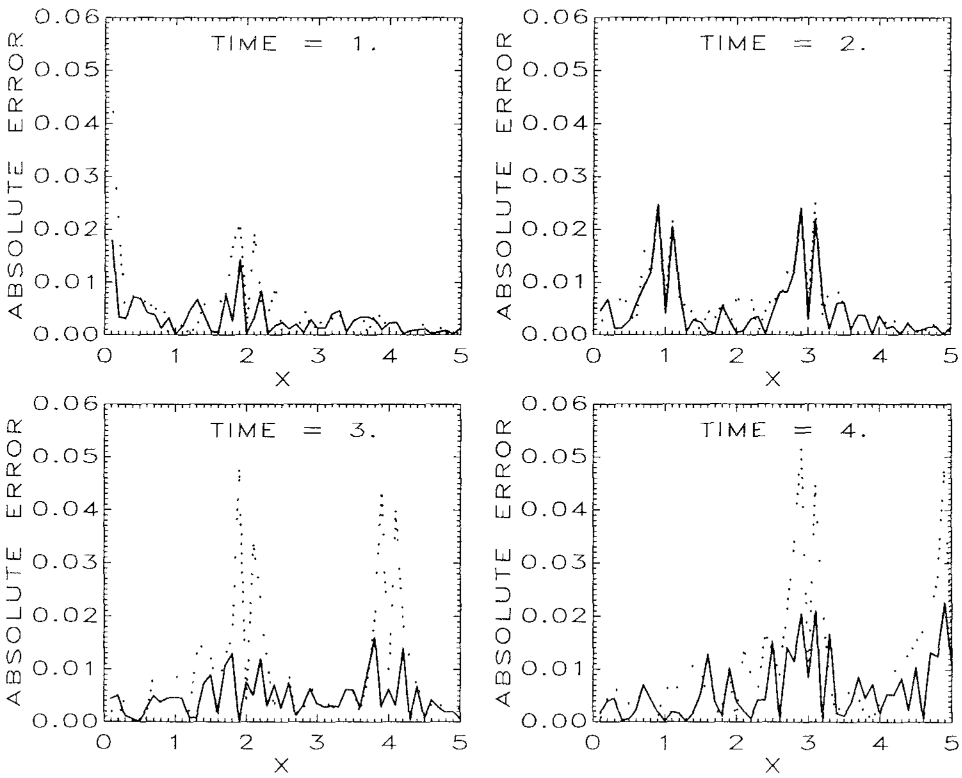

Fig. 16. The absolute value of the error between Weeks' method and the actual inverse for (16) as a function of x. The solid line is for $b = 2.1$; the dotted line, $b = 3.5$; and the dashed line, $b = 7.0$.

other hand, high degrees of precision will always require considerably more mathematical analysis.

5. CONCLUSIONS

In this paper we examined three popular methods to numerically invert Laplace transforms. The first method is a straightforward application of the trapezoidal rule to Bromwich's integral. This scheme was improved by Albrecht and Honig [1], by introducing corrections to reduce the discretization error and sequence accelerators to reduce the truncation error. The second method, developed by Weeks [22], integrates Bromwich's integral by using Laguerre polynomials. Finally, the third method, devised by Talbot [18], deformed Bromwich's contour so that it begins and ends in the third and second quadrant of the s-plane, respectively.

These three techniques were tested on transforms that are archetypical of those found in the scientific and engineering literature. For a proper choice of

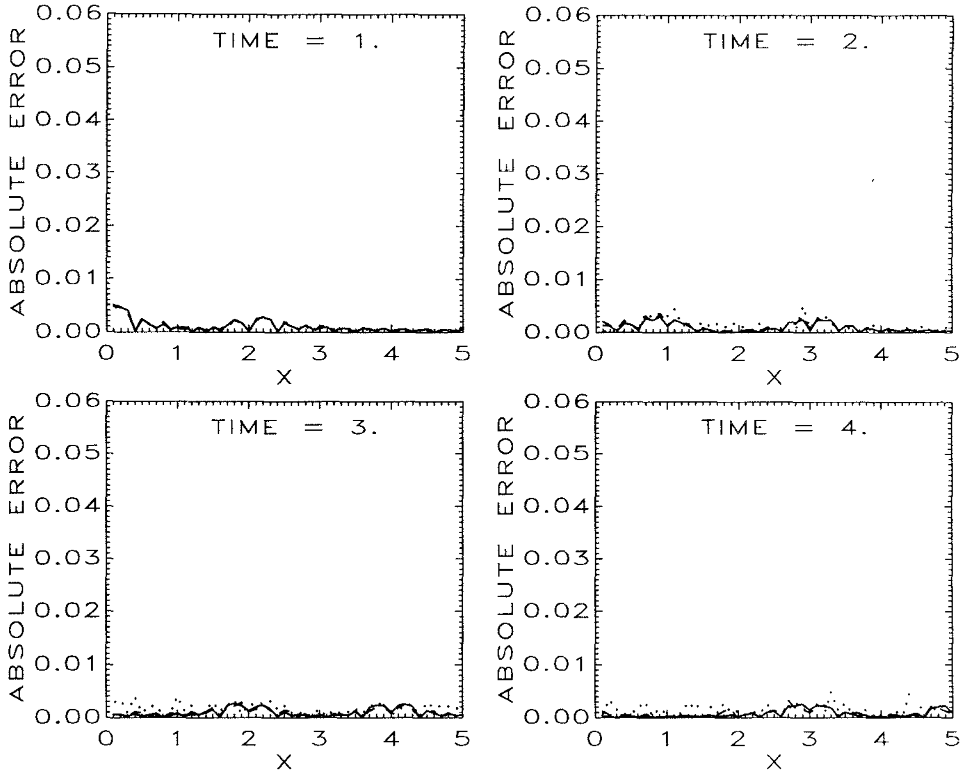

Fig. 17. The absolute value of the error between Talbot's method and the actual inverse for (16) as a function of x. The solid line is for the parameter σ predicted by subroutine TAPAR, the dotted line, when 5σ is used in Talbot's method and the dashed line, when $\sigma/5$ is used in Talbot's method.

parameters, all of the schemes give excellent results. Talbot's method, however, enjoys two special advantages over the direct integration and Weeks' methods. First, there are specific rules that allow for the optimal parameter values. Second, for a wide range of parameter values the error is remarkably constant as well as small. On the other hand, Talbot's method cannot be used if the singularities have imaginary parts that extend from $-\infty$ to ∞. Similar results were found in the case of joint Laplace-Fourier inversions. However, the errors were much larger because of the numerical integration involved in the numerical inversion of the Fourier transform.

As one might expect, when all of the methods give good results, the exact choice depends upon the problem. The Talbot scheme is very fast and the subroutine TAPAR did an excellent job of providing the optimum choice of required parameters. Unfortunately, the transform may only have singularities with a bounded imaginary part, and the nature and location may preclude a rapid, accurate inversion. When Talbot's method fails, the investi-

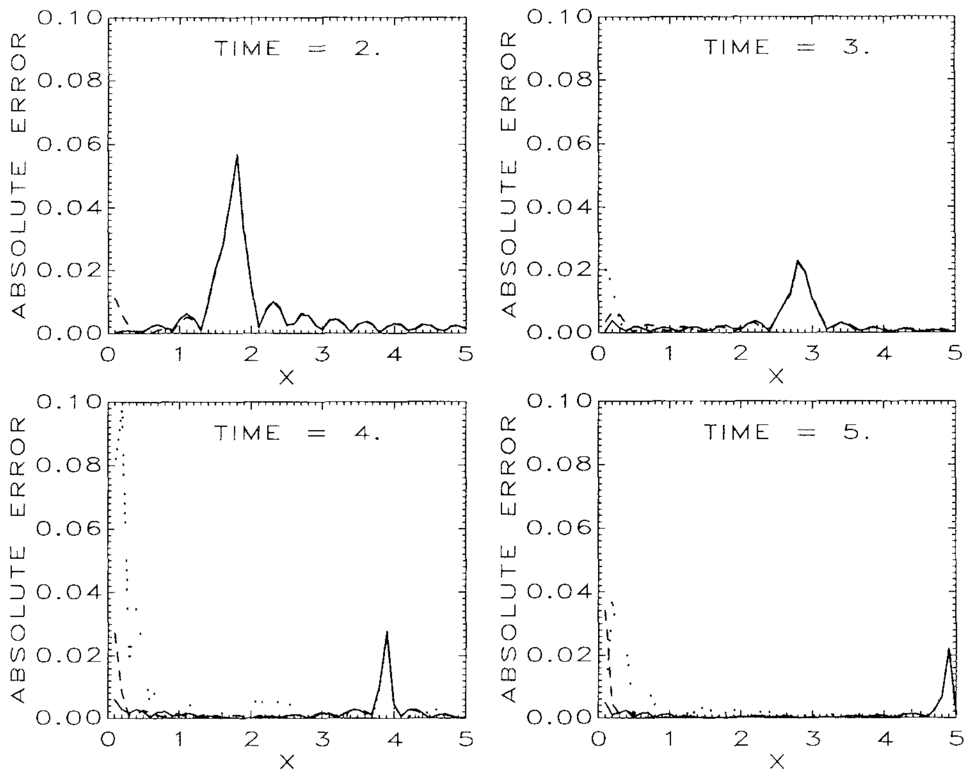

Fig. 18. Same as Figure 15, except for transform (19).

gator has a choice between the direct method using the Albrecht and Honig's [1] maximum/minimum method or Weeks' method. There is no compelling reason for choosing one method over the other, unless a large number of values of t are sought. Then Weeks' method is superior.

ACKNOWLEDGMENTS

The author thanks Wayne Higgins and Hendrik Tolman for their critical reading and many useful suggestions in developing this manuscript. The author would also like to thank the three anonymous reviewers for their many useful suggestions.

REFERENCES

1. ALBRECHT, P., AND HONIG, G. Numerische Inversion der Laplace-Transformierten. *Ang Inf. 19*, 8 (Aug. 1977), 336–345. In German.
2. BOLEY, B. A., AND CHAO, C. C. Some solutions of the Timoshenko beam equations. *J Appl. Mech 22*, 4 (Dec. 1955), 579–586

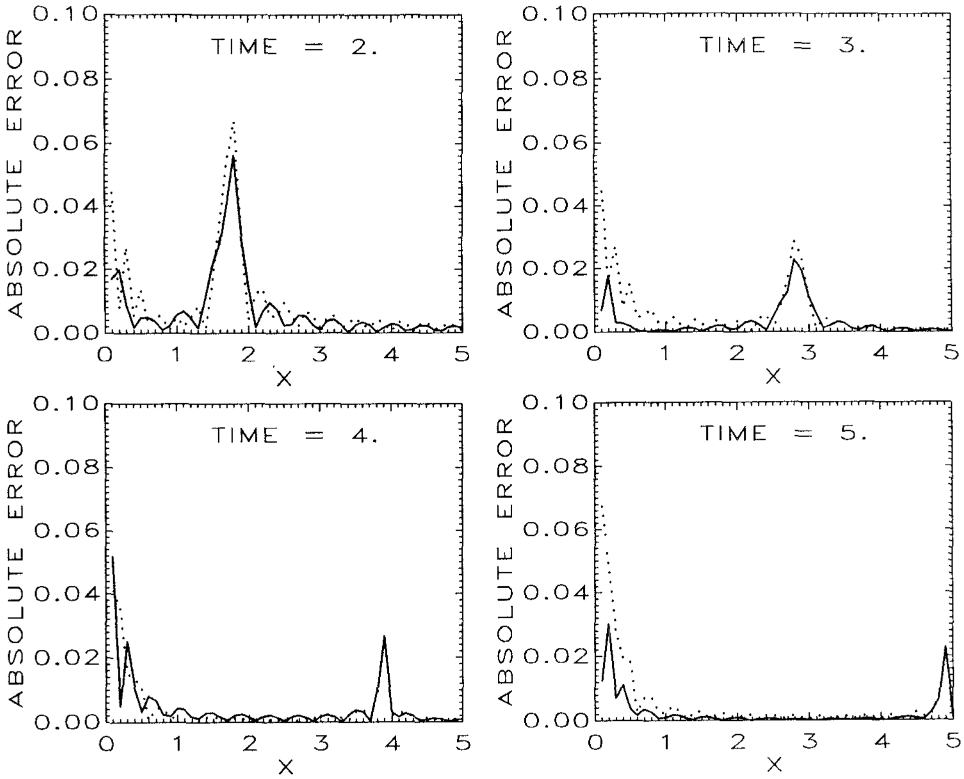

Fig. 19. Same as Figure 16, except for transform (19).

3. Crump, K. S. Numerical inversion of Laplace transforms using a Fourier series approximation. *J. ACM 23*, 1 (Jan. 1976), 89–96.
4. Davies, B., and Martin, B. Numerical inversion of the Laplace transform: A survey and comparison of methods. *J. Comput. Phys. 33*, 1 (Oct. 1979), 1–32.
5. De Hoog, F. R., Knight, J. H., and Stokes, A. N. An improved method for numerical inversion of Laplace transforms. *SIAM J. Sci. Stat. Comput. 3*, 3 (Sept. 1982), 357–366.
6. Garbow, B. S., Giunta, G., Lyness, J. N., and Murli, A. Software for an implementation of Weeks's method for the inverse Laplace transform problem. *ACM Trans. Math. Softw. 14*, 2 (June 1988), 163–170.
7. Garbow, B. S., Giunta, G., Lyness, J. N., and Murli, A. Algorithm 662: A FORTRAN software package for the numerical inversion of the Laplace transform based on Weeks' method. *ACM Trans. Math. Softw. 14*, 2 (June 1988), 171–176.
8. Giunta, G., Laccetti, G., and Rizzardi, M. More on the Weeks method for the numerical inversion of the Laplace transform. *Numer. Math. 54*, 2 (Nov. 1988), 193–200.
9. Goldman, S. *Laplace Transform Theory and Electrical Transients*. Dover, New York, 1966.
10. Honig, G., and Hirdes, U. Algorithm 27. A method for the numerical inversion of Laplace transforms. *J. Comput. Appl. Math. 10*, 1 (Jan. 1984), 113–132.
11. Levin, D. Development of nonlinear transformations for improving convergence of sequences. *Int. J. Comput. Math. 3*, 4 (Feb. 1973), 371–388.

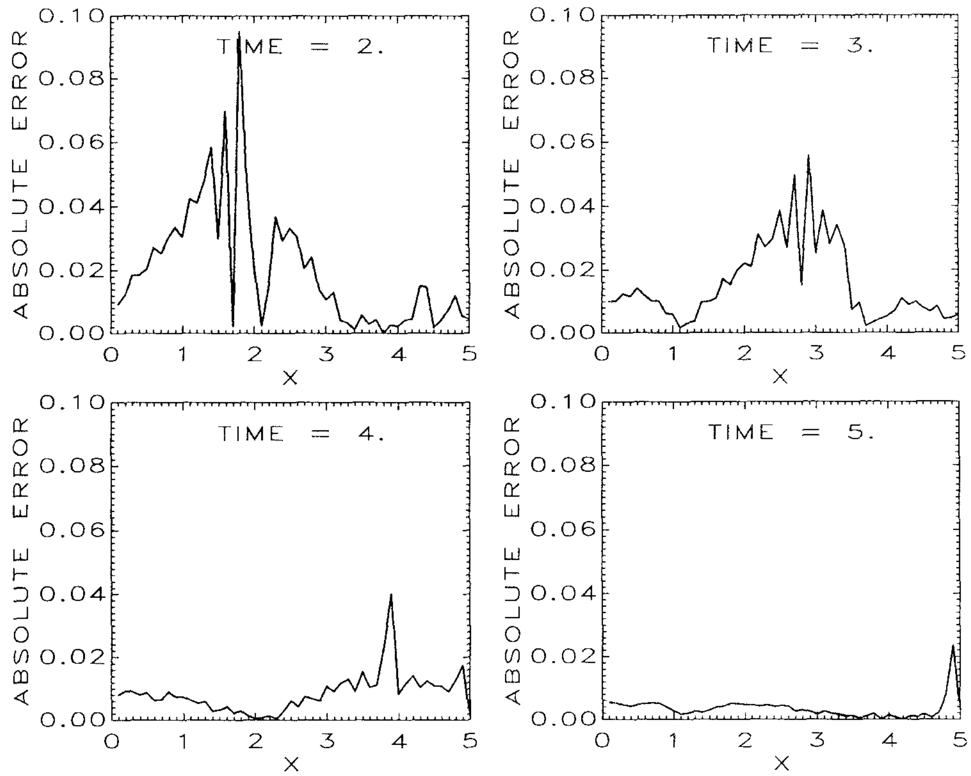

Fig. 20. Same as Figure 17, except for transform (19).

12. LYNESS, J. N., AND GIUNTA, G. A modification of the Weeks method for numerical inversion of the Laplace transform. *Math. Comput. 47*, 175 (July 1986), 313–322

13 MCLACHLAN, N. W. *Complex Variables and Operational Calculus.* 2nd ed., Macmillan, New York, 1953.

14. MURLI, A , AND RIZZARDI, M. Algorithm 682. Talbot's method for the Laplace inversion problem. *ACM Trans. Math. Softw. 16*, 2 (June 1990), 158–168

15. MUSGRAVE, M. J. P., AND TASI, J. Shock waves in diatomic chains. I. Linear analysis. *J Mech. Phys. Solids 24*, 1 (Mar. 1976), 19–42.

16. RIKITAKE, T., SATO, R., AND HAGIWARA, Y. *Applied Mathematics for Earth Scientists* D. Reidel, Boston, 1987.

17. SMITH, D. A., AND FORD, W. F. Numerical comparisons of nonlinear convergence accelerators. *Math. Comput. 38*, 158 (April 1982), 481–499.

18. TALBOT, A. The accurate numerical inversion of Laplace transforms. *J. Inst. Math. Appl. 23*, 1 (Jan. 1979), 97–120.

19. TANNER, R. I. Note on the Rayleigh problem for a visco-elastic fluid *ZAMP 13*, 6 (Nov. 1962), 573–580.

20. TING, T. C. T., AND SYMONDS, P. S. Longitudinal impact on viscoplastic rods—Linear stress-strain rate law. *J. Appl. Mech. 31*, 2 (June 1964), 199–207.

21. TSANG, L., AND RADER, D. Numerical evaluation of the transient acoustic waves form due to a point source in a fluid-filled bore-hole *Geophysics 44*, 10 (Oct. 1979), 1706–1720.

22. WEEKS, W. T. Numerical inversion of Laplace transforms using Laguerre functions. *J. ACM 13*, 3 (July 1966), 419–429.
23. WIMP, J. *Sequence Transformations and Their Applications*. Academic Press, New York, 1981.
24. WYNN, P. On a device for computing the $e_m(S_n)$ transformation. *MTAC 10* (1956), 91–96.

Received July 1991; revised June 1992; accepted June 1992